

PAPER DETAILS

TITLE: Numerical investigation of the effects of different baffle types on the thermal performance of a shell and tube heat exchanger

AUTHORS: Halil BAYRAM,Gökhan Sevilgen


PAGES: 58-66

ORIGINAL PDF URL: <https://dergipark.org.tr/tr/download/article-file/535075>


Numerical investigation of the effects of different baffle types on the thermal performance of a shell and tube heat exchanger

¹Halil Bayram, ^{*2}Gökhan Sevilgen

¹Department of Mechanical Engineering, Faculty of Technology, Amasya University, 05100, Amasya, TURKEY

halil.bayram@amasya.edu.tr, 

²Department of Automotive Engineering, Faculty of Engineering, Bursa Uludağ University, 16059, Bursa, TURKEY,

gsevilgen@uludag.edu.tr, 

Research Paper

Received Date: 21.02.2018

Accepted Date: 21.07.2018

Abstract

In this study, the thermal performance of a small scale shell and tube heat exchanger was performed according to the baffle type by using three dimensional Computational Fluid Dynamics (CFD) method. In numerical calculations, segmental and continuous helical baffle types were selected to get the comparative results. For helical baffle type, we used two different models that the numbers of helical rotations and baffle spacing length were different. Thus, we determined five different numerical models and the thermal performance of each models were evaluated under different inlet temperature values selected as 50, 60 and 70°C for the tube side. The inlet temperature value and the mass flow rate of shell side were kept constant during all the numerical calculations. The heat transfer calculations were achieved by using Logarithmic Mean Temperature Difference (LMTD) method. We also employed the Bell-Delaware method which can be used accurately for shell and tube heat exchangers. The highest thermal performance was determined in Case-IV which had equal baffle spacing and the maximum number of rotations for continuous helical baffle. The predicted total pressure drop results obtained from the numerical calculations were in good agreement with the calculated total pressure drop from Bell-Delaware method. The lowest pressure drop and the highest thermal performance were achieved for continuous helical baffle type compared to the segmental equal spacing baffle type. The numerical simulations based on CFD analysis can provide more information about heat exchangers and this tool can be used to improve both design and the thermal performance of heat exchangers.

Keywords: Shell and tube heat exchanger, helical baffle, segmental baffle, CFD

1. INTRODUCTION

The basic function of the heat exchanger is transfer energy from one fluid zone to another one and shell and tube heat exchangers are indirect contact types which are more suitable compared to the others in view of practical applications and maintenance [1, 2]. Thus, shell and tube heat exchanger is one of the common preferred types of heat exchanger which is used in different areas such as refrigeration, chemical process, manufacturing, power generation etc. [3-5]. There are number of classifications according to different parameters such as construction, number of fluids, flow arrangements etc. In shell and tube heat exchangers, there are two main flow region called shell and tube side flows. Shell side flow analysis is more complex than the tube side because different flow streams such as cross flow, by-pass and leakage were occurred in practice. To determine these streams, various parameters such as tube bundle layout, baffle design and shell side flow arrangements should be evaluated considering desired heat transfer rate and getting minimum pressure drop. Baffles are used to support tubes and to provide desirable velocity

distribution in shell side [2, 6]. Geometrical parameters of the baffle lead to make different flow streams at the shell side of the heat exchanger and baffles have different types such as segmental, helical, slotted etc. [1, 7, 8]. Segmental baffles are the most commonly used baffle type. On the other hand, heat exchangers with helical baffle have higher thermal performance than heat exchangers with segmental baffle at equal pressure drop values [9]. Helical baffles consist of two major types known as continuous and non-continuous [7]. A properly designed continuous helical baffled heat exchanger can decrease fouling, avoid vibration and enhance the thermal performance [10]. In available literature, there are too many studies about the effects of baffle parameters such as baffle type, baffle cut, baffles orientation angles, baffle inclination angle, helix angle etc. on the heat transfer rate and pressure [11-17]. But the researches include baffle spacing length are very limited. Moreover, selecting of right distance of two adjacent baffles can be used to improve the heat transfer rate. For instance, reducing the baffle spacing length lead to increase heat transfer rate but the pressure drop is increased too and so the pumping power. This adverse effect can be

*Corresponding Author: Address: Department of Automotive Engineering, Faculty of Engineering, Bursa Uludağ University, 16059, Bursa, TURKEY, gsevilgen@uludag.edu.tr , Phone: +90 224 294 2648

eliminated by using variable baffle spacing length in shell side which had nearly equal thermal performance compared to the heat exchanger with equal baffle spacing length [18].

In this paper, the thermal performance evaluation of an E type small scale shell and tube heat exchanger was carried out by numerical approach. To enhance the thermal performance and getting comparative results we developed five different CFD models considering with TEMA standards [19]. In the first model, a segmental baffle type with equal baffle spacing was chosen as a referenced model for getting improvements of this model. The continuous helical baffle with equal and variable baffle spacing length was selected in the second and third models, respectively. The numbers of helical rotations were selected as three in these models. In the fourth and fifth models, the numbers of helical rotations were increased to four and these models had also continuous helical baffle with equal and variable baffle spacing, respectively.

During the numerical calculations, the effect of the inlet temperature values of hot fluid on the thermal performance of a small scale heat exchanger were performed by using three dimensional CFD method. The numerical results based on simulations were integrated into the theoretical calculations of the heat exchanger by using LMTD method and we also compared the numerical results to the theoretical calculations obtained from Bell-Delaware method. All these computations were performed under steady-state conditions. The purpose of this study is to investigate both the design effects of baffle type and baffle spacing on the heat transfer rate and pressure drop. We also investigated numerically the impacts of the rating parameters such as mass flow rate and the inlet temperature value of fluid to get the better design in view of thermal efficiency in all cases.

2. MATERIALS AND METHODS

2.1. Theoretical study

Total heat transfer rate can be calculated considering energy conservation by using Equations (1 and 2). In these equations, the heat transfer between outer surfaces of the shell side and its surroundings is negligible and these surfaces assumed as adiabatic.

$$Q_h = (\dot{m} \cdot c_p)_h \cdot (T_{h,i} - T_{h,o}) \quad (1)$$

$$Q_c = (\dot{m} \cdot c_p)_c \cdot (T_{c,o} - T_{c,i}) \quad (2)$$

LMTD method is used for the calculation of the total heat transfer rate due to temperature variation with locations. The mass flow rate (\dot{m} - kg/s), specific heat (c_p - kJ/kgK), inlet and outlet temperature values for hot ($T_{h,i}$, $T_{h,o}$) and cold ($T_{c,i}$, $T_{c,o}$) fluid zones were used in Equations (1 and 2) so as to calculate the total heat transfer rate. This value can also be calculated by using Equation (3) and the terms of the equation were U (W/m²K), A (m²) and ΔT_{lm} named as

the total heat transfer coefficient, the total heat transfer area and the logarithmic temperature difference, respectively. Calculation of ΔT_{lm} depends on the flow direction and can be calculated by using Equations (4-6).

$$Q = U \cdot A \cdot \Delta T_{lm} \quad (3)$$

$$\text{For parallel flow; } \Delta T_1 = T_{h,i} - T_{c,i} \quad \Delta T_2 = T_{h,o} - T_{c,o} \quad (4)$$

$$\text{For counter flow; } \Delta T_1 = T_{h,i} - T_{c,o} \quad \Delta T_2 = T_{h,o} - T_{c,i} \quad (5)$$

$$\Delta T_{lm} = \frac{\Delta T_1 - \Delta T_2}{\ln(\Delta T_1 / \Delta T_2)} \quad (6)$$

For shell side heat transfer calculations, Kern and Bell-Delaware methods are commonly used. Kern method is used preliminary calculations and in this method Reynolds number calculations based on equivalent diameter. Baffle cut ratio is assumed as constant 25% in Kern method. However, this ratio changes between 15% and 45% according to TEMA standards. On the other hand, Bell-Delaware method is more complex than Kern method which takes into account baffle cut ratio, bypass and leakage streams on the shell side heat transfer coefficient and the total pressure drop.

Reynolds number is calculated by using outer diameter of tube in this method. The Bell-Delaware method can be used accurately for shell and tube heat exchanger which is designed according to TEMA standards. The detailed information about these methods can be found in references 2 and 4.

The shell side convection heat transfer coefficient (h_o) was calculated with using Equation (7) in Bell-Delaware method mentioned above. The J factors had important roles and all these j factors were assumed as one except J_b which is the correction factor for bundle bypassing. J_c is the correction factor for baffle cut and spacing was assumed as one because there were no tubes in the window area. J_r was assumed as one too. J_l is the correlation factor for baffle leakage effects including tube-to-baffle and shell-to-baffle leakage. But in the CFD calculations the leakage effects were not considered so J_l was assumed as one.

The last J factor, J_s is the correction factor for variable baffle spacing at the inlet and outlet zones of shell side. In the numerical calculations for Case-I, the baffle spacing was equal and J_s factor was taken as one. In the equation, h_{id} is the ideal heat transfer coefficient for pure crossflow in an ideal tube bank [6].

$$h_o = h_{id} J_c J_b J_s J_r \quad (7)$$

In tube side, to calculate the convective heat transfer coefficient (h_i) Petukhov-Kirillov correlation was used as given by Equation (8 and 9) (Kakaç, et al., 2012).

$$Nu = \frac{(f/2) Re Pr}{1.07 + 12.7 (f/2)^{1/2} (Pr^{2/3} - 1)} \quad (8)$$

$$f = (1.58 \ln Re - 3.28)^{-2} \quad (9)$$

The total heat transfer coefficient (U) was also calculated by using the Equation (10) with using convective heat transfer coefficient of both shell and tube sides, the tube diameter of inside and outside and the thermal conductivity of tube material [6].

$$U = \frac{d_o}{d_i} \frac{1}{h_i} + \frac{d_o \ln(d_o/d_i)}{2k_{tube}} + \frac{1}{h_o} \quad (10)$$

In Bell-Delaware method the shell side total pressure drop (Δp_s) can be calculated with the dividing shell side of the heat exchanger into four regions and each region was separately calculated to obtain the total pressure drop. The total pressure drop can be calculated from Equation (11) where, the pressure drop defined for internal cross-flow (Δp_c), baffle window (Δp_{win}), entering-leaving (Δp_e) and the nozzle (Δp_n) regions, respectively. More detailed information about the calculating the total pressure drop using Bell-Delaware method can be found in references [6, 18].

$$\Delta p_s = \Delta p_c + \Delta p_{win} + \Delta p_e + \Delta p_n \quad (11)$$

2.2. Numerical study

In the numerical simulations, we designed five different models by using three dimensional CFD method. These models were Case-I to Case-V and baffle type of Case-I was segmental and this case had equal baffle spacing length. This case was selected as a reference model which tube layout, baffle type, baffle cut ratio and baffle spacing were compatible with TEMA standards.

At the design stage of CAD model, tube layout angle was selected as 30° which has the greatest tube density. The heat exchanger had also 4 segmental baffles for Case-I and 7 tubes were designed for tube layout. The CAD models used in the numerical simulations of all cases are shown in Figure 1.

The first case had segmental baffle type with equal baffle spacing length. The second case had continuous helical baffle type with three numbers of rotations and equal baffle spacing length. The third case was similar to the second one but variable baffle spacing length was selected.

In the fourth and fifth cases number of helical rotations of baffle was determined as four and these models had also continuous helical baffle type with equal and variable baffle spacing length, respectively. The schematic view of all baffle spacing schemes and the dimensions used in the computations are shown Figure 2 and Table 1.

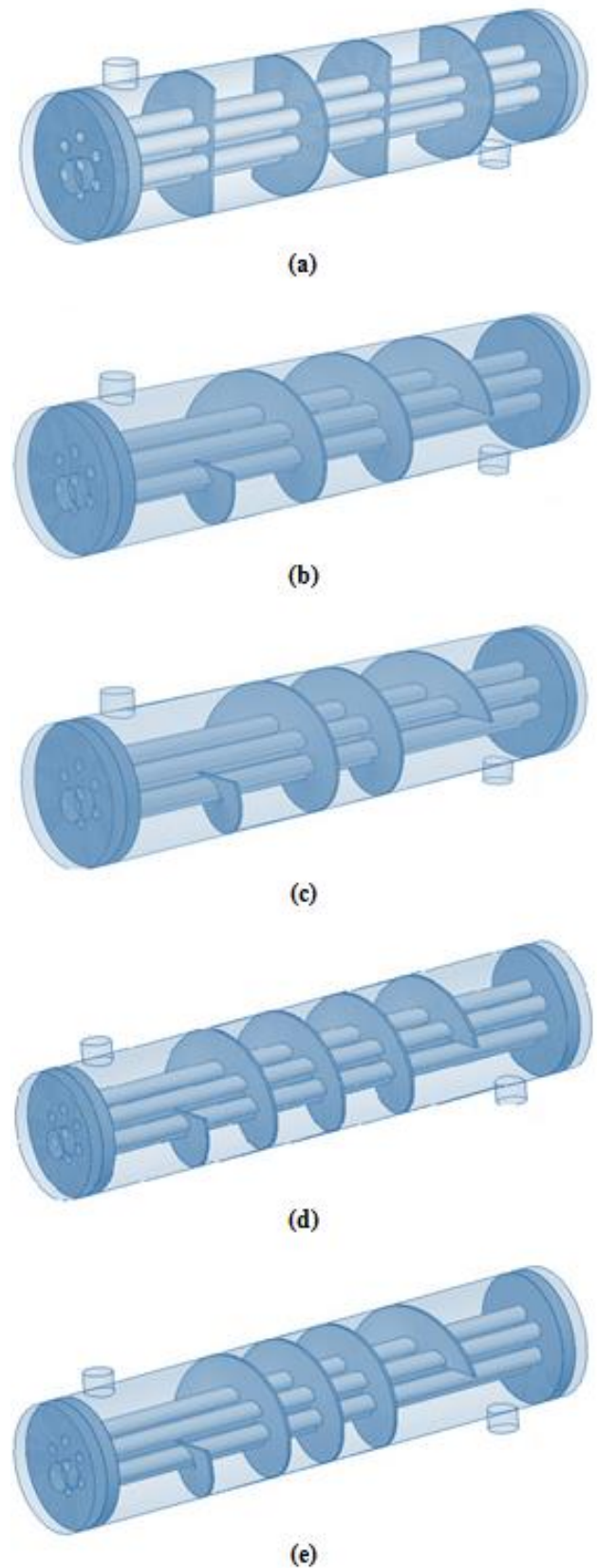


Figure 1. CAD model of small scale shell and tube heat exchanger (a) Case-I (b) Case-II (c) Case-III (d) Case-IV (e) Case-V

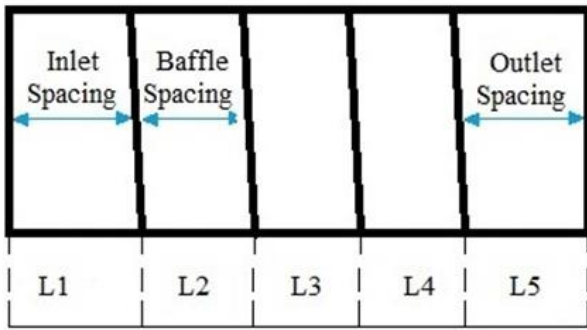


Figure 2. Schematic view of the dimensions of baffle spacing length

Table 1. The dimensions of baffle spacing length of all numerical cases

		Spacing length (mm)			
Spacing name	Case-I / Case-II	Case-III	Case-IV	Case-V	
L1	36.0	36.0	36.0	36.0	
L2	36.0	40.5	26.75	32.5	
L3	36.0	27.0	26.75	21.0	
L4	36.0	40.5	26.75	21.0	
L5	36.0	36.0	26.75	32.5	
L6	-	-	36.0	36.0	

In the numerical calculations, mesh generation is very crucial step for pre-processing to obtain high precision numerical results. The surface mesh structure of the all

cases were similar each other and is shown in Figure 3 for Case-III. Computational domains include about 3×10^6 cells and ANSYS-Fluent software package was used for all numerical calculations. This software solves continuum, energy and transport equations numerically and the governing equations can be written in Equations (12-17) [4].

Conservation of mass:

$$\nabla \cdot (\rho \vec{V}) = 0 \quad (12)$$

x-momentum:

$$\nabla \cdot (\rho u \vec{V}) = -\frac{\partial p}{\partial x} + \frac{\partial \tau_{xx}}{\partial x} + \frac{\partial \tau_{yx}}{\partial y} + \frac{\partial \tau_{zx}}{\partial z} \quad (13)$$

y-momentum:

$$\nabla \cdot (\rho v \vec{V}) = -\frac{\partial p}{\partial y} + \frac{\partial \tau_{xy}}{\partial x} + \frac{\partial \tau_{yy}}{\partial y} + \frac{\partial \tau_{zy}}{\partial z} + \rho g \quad (14)$$

z-momentum:

$$\nabla \cdot (\rho w \vec{V}) = -\frac{\partial p}{\partial z} + \frac{\partial \tau_{xz}}{\partial x} + \frac{\partial \tau_{yz}}{\partial y} + \frac{\partial \tau_{zz}}{\partial z} \quad (15)$$

Energy:

$$\nabla \cdot (\rho e \vec{V}) = -p \nabla \cdot \vec{V} + \nabla \cdot (k \nabla T) + q + \Phi \quad (16)$$

In Equation (16), Φ is the dissipation function that was described in Equation (17).

$$\Phi = \mu \left[2 \left[\left(\frac{\partial u}{\partial x} \right)^2 + \left(\frac{\partial v}{\partial y} \right)^2 + \left(\frac{\partial w}{\partial z} \right)^2 \right] + \left(\frac{\partial v}{\partial x} + \frac{\partial u}{\partial y} \right)^2 + \left(\frac{\partial w}{\partial y} + \frac{\partial v}{\partial z} \right)^2 + \left(\frac{\partial u}{\partial z} + \frac{\partial w}{\partial x} \right)^2 \right] + \lambda (\nabla \cdot \vec{V})^2 \quad (17)$$

Table 2. Solver settings and boundary conditions used in the numerical simulations

Solver settings	
Solver	Pressure-based
Time	Steady-state conditions
Equations	Combined simulation of flow and energy
Flow type	k-epsilon Standard turbulence model
Shell side	
Supply temperature of cold water	20 °C
Mass flow rate	0.4 kg s ⁻¹
Shell outer surfaces	Adiabatic conditions
Outlet nozzle	Gauge pressure equals to 0 Pa
Tube side	
Supply temperature of hot water	50 °C / 60 °C / 70 °C
Mass flow rate	0.2 kg s ⁻¹
Outlet surfaces of the tube side	Gauge pressure equals to 0 Pa



Figure 3. Isometric view of mesh structure of the heat exchanger (Case-III)

Water was selected as a fluid for both shell and tube side for the numerical calculations. The mass flow rates were kept constant as a value of 0.2 kg s^{-1} and 0.4 kg s^{-1} for hot and cold side, respectively for all cases. Inlet temperature value of the tube side was adjusted 50°C , 60°C and 70°C .

Inlet temperature value of shell side was remained unchanged and it was a value of 20°C for all numerical simulations. Table 2 shows the boundary conditions and solver settings used in the numerical calculations.

3. RESULTS AND DISCUSSIONS

The calculated temperature values at the outlet surface of both shell and tube sides are shown in Table 3. According to the numerical results, the temperature values obtained for continuous helical baffle type with three numbers of rotations (Case-II and Case-III) were equal.

Computed outlet surface temperature values of the tube side for segmental baffle type were higher than helical ones in general. The heat exchangers with helical baffle have higher shell side outlet temperature values than segmental ones.

Table 3. Outlet temperature values for all numerical cases ($^\circ\text{C}$)

Baffle type	Computed temperature values at outlet surfaces of both tube and shell sides									
	Segmental				Continuous Helical					
	0		3		3		4		4	
Number of rotations	(Case-I)		(Case-II)		(Case-III)		(Case-IV)		(Case-V)	
Tube side inlet temperature values ($^\circ\text{C}$)	Tube side	Shell side	Tube side	Shell side	Tube side	Shell side	Tube side	Shell side	Tube side	Shell side
50	47.11	21.44	46.88	21.55	46.88	21.55	46.78	21.60	46.79	21.59
60	56.15	21.92	55.84	22.07	55.84	22.07	55.70	22.14	55.72	22.12
70	65.18	22.40	64.80	22.58	64.80	22.58	64.63	22.67	64.55	22.65

From these results, we can easily say that the computed temperature difference between helical and segmental baffle type of heat exchangers increase with the rising of the tube side inlet temperature value. This means that helical baffle type heat exchanger had better performance for higher supply temperature values. The total heat transfer rate values obtained from theoretical calculations based on numerical results are shown in Table 4. The cases of heat exchanger with helical baffle have higher total heat transfer rate values than segmental ones. For the cases of equal baffle spacing, higher total heat transfer rate values were

predicted than the cases which had variable baffle spacing. But, increasing the number of helical rotations lead to rising in the total heat transfer rate of shell and tube heat exchangers. The maximum heat transfer rate was calculated for Case-IV which had equal baffle spacing with maximum number of rotations for continuous helical baffle and the increase in total heat transfer rate was computed about 11.6% in percentage compared to the Case-I which had segmental baffle type.

Table 4. Numerical results of the total heat transfer rate (W) for all models and comparison to the data obtained for segmental baffle type

Baffle type		Total heat transfer rate (W)				
		Segmental	Continuous Helical			
		0	3	3	4	4
Number of rotations		(Case-I)	(Case-II)	(Case-III)	(Case-IV)	(Case-V)
Tube side inlet temp. values ($^\circ\text{C}$)						
50	Q_{total}	2416.78	2610.27	2610.44	2695.87	2684.33
	(Increment)	0.0 %	+ 8.0 %	+ 8.0 %	+ 11.5 %	+ 11.1 %
60	Q_{total}	3223.87	3483.00	3483.26	3597.22	3581.90
	(Increment)	0.0 %	+ 8.0 %	+ 8.0 %	+ 11.6 %	+ 11.1 %
70	Q_{total}	4034.06	4358.12	4358.34	4501.94	4481.74
	(Increment)	0.0 %	+ 8.0 %	+ 8.0 %	+ 11.6 %	+ 11.1 %

The predicted temperature distributions at the middle section plane of the shell side for Case-IV are shown in Figure 4 which includes all inlet temperature values (Figure 4a-4c) of hot water. Predicted temperature distributions were obtained very similar for all numerical cases however, the temperature values were increased according to selected higher inlet temperature values.

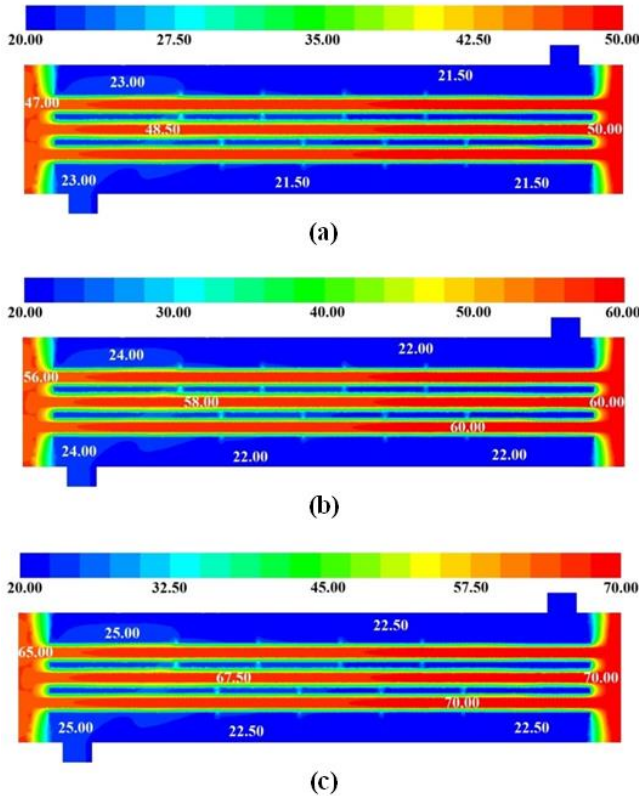


Figure 4. Temperature distribution at the center plane of the inlet temperature of hot water is (a)50°C (b)60°C (c)70°C (Case-IV)

The outlet temperature values obtained from the CFD calculations were used to determine the total heat transfer

coefficient (U). It was estimated nearly about 3580 $\text{Wm}^{-2}\text{K}^{-1}$ for all hot water inlet temperature values in CFD calculations. U was also calculated by using the Bell-Delaware method and it was about 3698 $\text{Wm}^{-2}\text{K}^{-1}$. These values were close to each other and the calculated U values for all cases are shown in Table 5.

Table 5. Results of numerical and analytical calculations for segmental baffle type

	Inlet temperature of hot water	CFD	Bell-Delaware
U ($\text{W m}^{-2} \text{K}^{-1}$)	50°C	3578.98	3698
	60°C	3577.26	
	70°C	3580.35	

The total pressure drop obtained from CFD results, are shown in Table 6. As expected, the total pressure drop between inlet and outlet surfaces of the shell side was decreased for shell and tube heat exchangers with helical baffle type. The maximum pressure drop was achieved for segmental baffle type.

The total pressure drop values obtained from Bell-Delaware and CFD methods of shell and tube heat exchanger with segmental baffles were approximately 32430 Pa and 34745 Pa, respectively. The difference between these values was acceptable for the design stage and computed about 7% in percentage. On the other hand, the calculated total pressure drop was increased with the number of helical rotations according to results shown in Table 6. In general, the cases used variable baffle spacing had higher pressure drops compared to the cases which had equal baffle spacing for helical shell and tube heat exchangers. The total pressure drop obtained for Case-II which had helical baffle type with equal baffle spacing was calculated about 26 kPa for all numerical calculations. The decrease in percentage of computed pressure drop for this case was about 25% compared to the Case-I which had segmental baffle type. Another important result is that the number of helical rotations increased the total pressure drop in general.

Table 6. Numerical results of the shell side total pressure drop (Pa) for all models and comparison to the data obtained for segmental baffle type

		Total pressure drop (Pa)				
Baffle type		Segmental		Continuous helical		
Number of rotations		0 (Case-I)	3 (Case-II)	3 (Case-III)	4 (Case-IV)	4 (Case-V)
Tube side inlet temp. values (°C)	Bell-Delaware	CFD results				
50	ΔP_{total}	34707	26104	26447	28288	28781
	(Decrement)	0.0%	- 24.8%	- 23.8%	- 18.5%	- 17.1%
60	ΔP_{total}	34765	26105	26447	28276	28781
	(Decrement)	0.0%	- 24.9%	- 23.9%	- 18.7%	- 17.2%
70	ΔP_{total}	34764	26105	26447	28289	28781
	(Decrement)	0.0%	- 24.9%	- 23.9%	- 18.6%	- 17.2%

The computed velocity distributions for all numerical models are shown in Figure 5 and the flow streams obtained for segmental baffle type had zigzag manner across the tube bundle, however, using helical baffle type makes the flow stream rotational and spiral that leads to get lower pressure drop values. The computed velocity values were ranged from 0 m/s to 1.8 m/s in shell side in general and the this value was calculated about 5.2 m/s in the nozzle region due to contraction of sections.

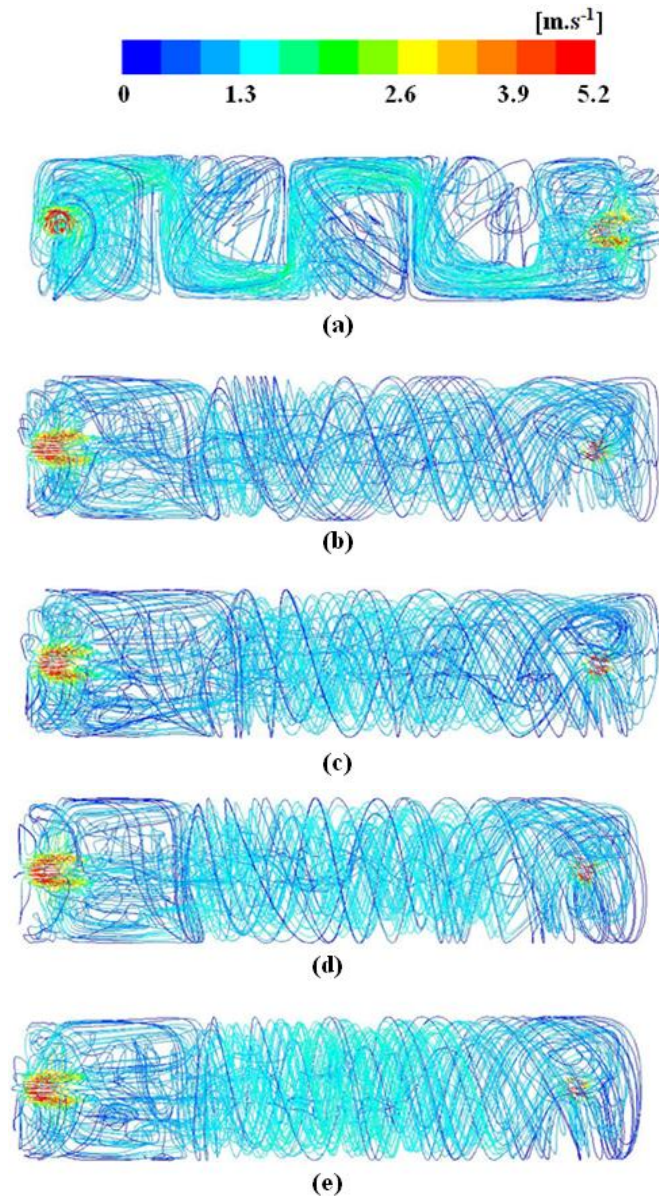


Figure 5. Velocity distributions of shell side flow (a)Case-I (b)Case-II (c)Case-III (d)Case-IV (e)Case-V

4. CONCLUSIONS

In this study, the thermal performance evaluation of an E type small scale shell and tube heat exchanger was carried out by using three dimensional CFD method considering baffle type and baffle spacing under different tube side inlet temperature values. To enhance the thermal performance

and getting comparative results we developed different CFD models. The numerical results based on simulations were integrated into the theoretical calculations of the heat exchanger by using LMTD method. We also employed the Bell-Delaware method which can be used accurately for shell and tube heat exchangers. According to the numerical simulations, the main results are described below:

- Case-IV, which had equal baffle spacing and the maximum number of helical rotations (four) had the highest thermal performance.
- Increasing the number of helical rotations can cause increase in the total heat transfer rate however, it also increase the total pressure drop. So, the number of helical rotations had great effect on the thermal performance of shell and tube heat exchanger.
- For the same mass flow rate, the thermal performances of the heat exchangers with helical baffle type had higher than the model which had segmental type in general.
- According to the comparison of numerical and theoretical calculations, it was observed that the total heat transfer coefficient values of CFD and Bell-Delaware results were close to each other. These two methods can be used together to evaluate the thermal performance of shell and tube heat exchangers. Moreover, the theoretical methods such as Kern and Bell-Delaware do not give any information about the location of leakage and by pass streams but CFD method was utilized for such flow patterns.
- The total pressure drop values of heat exchanger model with equal baffle spacing were lower than variable ones and the lowest total pressure drop was achieved for Case-II which had equal baffle spacing with helical baffle type.
- The total pressure drop values obtained from the theoretical calculations with using Bell-Delaware method and numerical calculations were close to each other.
- The flow pattern in shell side for segmental baffle had zigzag manner across the tube bundle, however, using helical baffle type makes this pattern rotational and spiral that leads to get lower pressure drop values.
- The decrease in percentage of computed pressure drop for Case-II was about 25% compared to the Case-I which had segmental baffle type.
- The helical baffle type heat exchanger was an alternative model and can be replaced with segmental type for industrial applications.
- Therefore, the baffle configuration design can be used to ensure better thermal performance and also reduced the total pressure drop.
- CFD tool can be used for improving thermal efficiency of shell and tube heat exchanger and this tool can provide more information about leakage and bypass streams and dead zones of shell and tube heat exchangers.

NOMENCLATURE

A	total heat transfer area	$[m^2]$
c_p	specific heat at constant pressure	$[J.kg^{-1}.K^{-1}]$
d_i	tube inside diameter	$[m]$
d_o	tube outside diameter	$[m]$
f	friction factor	-

g	gravitational acceleration	$[\text{m.s}^{-2}]$
h	heat transfer coefficient	$[\text{W.m}^{-2}\text{K}^{-1}]$
j_i	Colburn j-factor for an ideal tube bank	-
J_b	bundle bypass correction factor	-
J_c	segmental baffle window correction factor	-
J_l	baffle leakage correction factor	-
J_r	laminar flow heat transfer correction factor	-
J_s	heat transfer correction factor for unequal end baffle spacing	-
k	thermal conductivity of fluid	$[\text{W.m}^{-1}\text{K}^{-1}]$
k_{tube}	thermal conductivity of tube material	$[\text{W.m}^{-1}\text{K}^{-1}]$
\dot{m}	mass flow rate	$[\text{kg.s}^{-1}]$
Nu	Nusselt number	-
p	pressure	$[\text{Pa}]$
Pr	Prandtl number	-
Q	total heat transfer rate	$[\text{W}]$
Re	Reynolds number	-
T	temperature	$[\text{K}]$
u, v, w	velocity components	$[\text{m.s}^{-1}]$
U	total heat transfer coefficient	$[\text{W.m}^{-2}\text{K}^{-1}]$
\vec{V}	velocity vector	-
x, y, z	position coordinates	-
Δp_s	total pressure drop for shell side	$[\text{Pa}]$
Δp_e	pressure drop in entering and leaving regions	$[\text{Pa}]$
Δp_c	pressure drop in internal cross flow region	$[\text{Pa}]$
Δp_w	pressure drop in window region	$[\text{Pa}]$
Δp_n	pressure drop in nozzle region	$[\text{Pa}]$
λ	second viscosity coefficient	-
ρ	density	$[\text{kg.m}^{-3}]$
τ	shear stress	$[\text{N.m}^{-2}]$
Φ	dissipation function	-
μ	dynamic viscosity	$[\text{N.s.m}^{-2}]$

Subscripts

c	cold
h	hot
i	inner
lm	logarithmic mean
o	outer

REFERENCES

[1] J.-F. Zhang, Y.-L. He, and W.-Q. Tao, "3D numerical simulation on shell-and-tube heat exchangers with middle-overlapped helical baffles and continuous baffles – Part I: Numerical model and results of whole heat exchanger with middle-overlapped helical baffles," *International Journal of Heat and Mass Transfer*, vol. 52, no. 23–24, pp. 5371–5380, Nov. 2009.

[2] R.K. Shah, D.P. Sekulic, *Fundamentals of heat exchanger design*, John Wiley & Sons, Inc., New Jersey, 2003.

[3] R. Selbaş, Ö. Kızılkın, and M. Reppich, "A new design approach for shell-and-tube heat exchangers using genetic algorithms from economic point of view," *Chemical*

Engineering and Processing: Process Intensification, vol. 45, no. 4, pp. 268–275, Apr. 2006.

[4] E. Ozden and I. Tari, "Shell side CFD analysis of a small shell-and-tube heat exchanger," *Energy Conversion and Management*, vol. 51, no. 5, pp. 1004–1014, May 2010.

[5] B. Parikshit, K. R. Spandana, V. Krishna, T. R. Seetharam, and K. N. Seetharamu, "A simple method to calculate shell side fluid pressure drop in a shell and tube heat exchanger," *International Journal of Heat and Mass Transfer*, vol. 84, pp. 700–712, May 2015.

[6] S. Kakaç, H. Liu, A. Pramuanjaroenkij, *Heat exchangers: selection, rating, and thermal design*, CRC Press: Florida, 2012.

[7] F. Nemati Taher, S. Zeynnejad Movassag, K. Razmi, and R. Tasouji Azar, "Baffle space impact on the performance of helical baffle shell and tube heat exchangers," *Applied Thermal Engineering*, vol. 44, pp. 143–149, Nov. 2012.

[8] J. Yang, L. Ma, J. Bock, A. M. Jacobi, and W. Liu, "A comparison of four numerical modeling approaches for enhanced shell-and-tube heat exchangers with experimental validation," *Applied Thermal Engineering*, vol. 65, no. 1–2, pp. 369–383, Apr. 2014.

[9] Q. Wang, G. Chen, Q. Chen, M. Zeng, and D. Zhang, "Numerical Studies of a Novel Combined Multiple Shell-Pass Shell-and-Tube Heat Exchanger With Helical Baffles," *Heat Transfer: Volume 2*, 2008.

[10] B. Peng, Q. W. Wang, C. Zhang, G. N. Xie, L. Q. Luo, Q. Y. Chen, and M. Zeng, "An Experimental Study of Shell-and-Tube Heat Exchangers With Continuous Helical Baffles," *Journal of Heat Transfer*, vol. 129, no. 10, p. 1425, 2007.

[11] Y.-G. Lei, Y.-L. He, R. Li, and Y.-F. Gao, "Effects of baffle inclination angle on flow and heat transfer of a heat exchanger with helical baffles," *Chemical Engineering and Processing: Process Intensification*, vol. 47, no. 12, pp. 2336–2345, Nov. 2008.

[12] K. Raj and S. Ganne, "Shell side numerical analysis of a shell and tube heat exchanger considering the effects of baffle inclination angle on fluid flow using CFD," *Thermal Science*, vol. 16, no. 4, pp. 1165–1174, 2012.

[13] X. Xiao, L. Zhang, X. Li, B. Jiang, X. Yang, and Y. Xia, "Numerical investigation of helical baffles heat exchanger with different Prandtl number fluids," *International Journal of Heat and Mass Transfer*, vol. 63, pp. 434–444, Aug. 2013.

[14] A. S. Ambekar, R. Sivakumar, N. Anantharaman, and M. Vivekenandan, "CFD simulation study of shell and tube heat exchangers with different baffle segment configurations," *Applied Thermal Engineering*, vol. 108, pp. 999–1007, Sep. 2016.

[15] A. El Maakoul, A. Laknizi, S. Saadeddine, M. El Metoui, A. Zaite, M. Meziane, and A. Ben Abdellah, "Numerical comparison of shell-side performance for shell and tube heat exchangers with trefoil-hole, helical and segmental baffles," *Applied Thermal Engineering*, vol. 109, pp. 175–185, Oct. 2016.

[16] Z. Ling, Z. He, T. Xu, X. Fang, X. Gao, and Z. Zhang, "Experimental and Numerical Investigation on Non-

Newtonian Nanofluids Flowing in Shell Side of Helical Baffled Heat Exchanger Combined with Elliptic Tubes,” *Applied Sciences*, vol. 7, no. 12, p. 48, Jan. 2017.

[17] M. Mellal, R. Benzeguir, D. Sahel, and H. Ameer, “Hydro-thermal shell-side performance evaluation of a shell and tube heat exchanger under different baffle arrangement and orientation,” *International Journal of*

Thermal Sciences, vol. 121, pp. 138–149, Nov. 2017.

[18] H. Bayram and G. Sevilgen, “Numerical Investigation of the Effect of Variable Baffle Spacing on the Thermal Performance of a Shell and Tube Heat Exchanger,” *Energies*, vol. 10, no. 12, p. 1156, Aug. 2017.

[19] TEMA, Standards of the tubular exchanger manufacturers association, Tubular Exchanger Manufacturers Association Inc., New York, 1999.